Well-Defined Ruthenium Olefin Metathesis Catalysts: Mechanism and Activity

Eric L. Dias, SonBinh T. Nguyen, and Robert H. Grubbs*

Contribution from The Arnold and Mabel Beckman Laboratory of Chemical Synthesis, Division of Chemistry And Chemical Engineering, California Institute of Technology, Pasadena, California 91125

Received September 6, 1996[⊗]

Abstract: Several ruthenium-based olefin metathesis catalysts of the formula $(PR_3)_2X_2Ru{=}CHCHCPh_2$ have been synthesized, and relative catalyst activities were determined by monitoring the ring-closing metathesis of the acyclic diene diethyl diallylmalonate. The following order of increasing activity was determined: X = I < Br < Cl and $PR_3 = PPh_3 \ll P^iPr_2Ph < PCy_2Ph < P^iPr_3 < PCy_3$. Additional studies were conducted with the catalyst $(PCy_3)_2Cl_2Ru{=}CH_2$ to probe the mechanism of olefin metathesis by this class of catalysts. The data support a scheme in which there are two competing pathways: the dominant one in which a phosphine dissociates from the ruthenium center and a minor one in which both phosphines remain bound. Higher catalyst activites could be achieved by the addition of CuCl to the reaction.

Introduction

The synthesis and isolation of the ruthenium vinylcarbene **1** opened the door to the development of well-defined, late transition metal, low oxidation state complexes that catalyze olefin metathesis.[1] In addition to the activity of **1** in the metathesis of strained cyclic[1,2] and exocyclic[3] olefins, the remarkable functional group tolerance and stability toward several conditions such as air, water, and acids[1] has made this class of catalyst particularly attractive for practical applications.

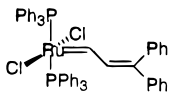

1

By exchanging the triphenylphosphines in **1** for tricyclohexylphosphines, it was found that the catalyst **2a** could also be easily synthesized and isolated.[4] However, **2a** proved to be a much more active catalyst than **1**, reacting with relatively low-strain cyclic olefins[4,5] as well as straight-chain alkenes,[4] while retaining the stability of **1** toward air and protic media.[4] The ring-closing metathesis of functionalized α,ω-dienes to produce five-, six-, seven-,[6,7] and eight-membered rings,[7,8] as well as macrocycles and covalently stabilized β-turns,[7] and likewise *ene*−*yne*−*ene* systems to make fused or tethered bicyclic molecules[9] are examples of the particular reactivity and synthetic utility of these catalysts.[10]

Scheme 1

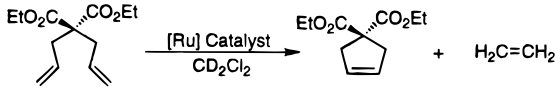

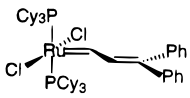

2a

Until now, a systematic investigation of the factors governing catalyst activity and the mechanism by which these catalysts perform olefin metathesis has not been reported. The present study was undertaken to address both of these topics in the following ways. By varying the ligand sphere around the ruthenium catalyst, we wished to determine how the electronic and steric properties of the ligands affect catalyst activity. Likewise, by examining the kinetics of olefin metathesis, we hoped to gain some insight as to the mechanistic pathway(s) by which these catalysts operate. Once the relationship between the mechanism, ligands, and catalyst activity was understood, we sought to apply this knowledge and tune catalyst activity in a desired fashion.

Results and Discussion

To determine the relative activities of the ruthenium catalysts, the ring-closing metathesis of commercially available diethyl diallylmalonate was studied, as shown in Scheme 1. Diethyl diallylmalonate was chosen as the substrate for two reasons: (1) it has been observed that ring-closing metathesis to the corresponding cyclopentene diester is quantitative and relatively

[⊗] Abstract published in *Advance ACS Abstracts,* April 1, 1997.

(1) Nguyen, S. T.; Johnson, L. K.; Grubbs, R. H. *J. Am. Chem. Soc.* **1992**, *114*, 3974−3975.

(2) Wu, Z.; Benedicto, A. D.; Grubbs, R. H. *Macromolecules* **1993**, *26*, 4975−4977.

(3) Wu, Z.; Nguyen, S. T.; Grubbs, R. H.; Ziller, J. W. *J. Am. Chem. Soc.* **1995**, *117*, 5503−5511.

(4) Nguyen, S. T.; Grubbs, R. H.; Ziller, J. W. *J. Am. Chem. Soc.* **1993**, *115*, 9858−9859.

(5) Hillmyer, M. A.; Laredo, W. R.; Grubbs, R. H. *Macromolecules* **1995**, *28*, 6311−6316.

(6) (a) Holder, S.; Blechert, S. *Synlett* **1996**, *June*, 505−506. (b) Crimmins, M. T.; King, B. W. *J. Org. Chem.* **1996**, *61*, 4192−4193. (c) Garro-Helion, F.; Guibe, F. *Chem. Commun.* **1996**, 641−642. (d) Fu, G. C.; Nguyen, S. T.; Grubbs, R. H. *J. Am. Chem. Soc.* **1993**, *115*, 9856−9857.

(7) (a) Furstner, A.; Langemann, K. *J. Org. Chem.* **1996**, *61*, 3942−3943. (b) Miller, S. J.; Grubbs, R. H. *J. Am. Chem. Soc.* **1995**, *117*, 5855−5856. (c) Borer, B.; Deerenberg, S.; Bieraugel, H.; Pandit, U. K. *Tetrahedron Lett.* **1994**, *35*, 3191−3194.

(8) Miller, S. J.; Kim, S.-H.; Chen, Z.-R.; Grubbs, R. H. *J. Am. Chem. Soc.* **1995**, *117*, 2108−2109.

(9) Kim, S.-H.; Bowden, N.; Grubbs, R. H. *J. Am. Chem. Soc.* **1994**, *116*, 10801−10802.

(10) For a recent review of olefin metathesis catalysts in organic synthesis, see Grubbs, R. H.; Miller, S. J.; Fu, G. C. *Acc. Chem. Res.* **1995**, *28*, 446−452.

S0002-7863(96)03136-8 CCC: $14.00

Table 1. Relative Activities of the Catalysts $(PR_3)_2X_2Ru{=}CH{-}CH{=}CPh_2$ in the Ring-Closing Metathesis of Diethyl Diallylmalonate[a]

catalyst	PR_3	X	activity (turnovers/h)[b]
2a	PCy_3	Cl	19.0
2b		Br	15.4
2c		I	1.4
3a	PCy_2Ph	Cl	8.0
3b		Br	4.5
3c		I	*c*
4a	P^iPr_3	Cl	17.5
4b		Br	13.9
4c		I	1.1
5a	P^iPr_2Ph	Cl	5.5
5b		Br	2.3
5c		I	*c*

[a] Conditions: [diethyl diallylmalonate]$_0$ = 0.2 M; [catalyst] = 0.010 M; temperature = 20 °C. [b] Turnover numbers were obtained by fitting data of [product] vs time to a double-exponential expression (see Figure 1) and using the product concentration from the 1-h time point of the curve fit. [c] Catalyst showed no activity in the metathesis reaction over several hours.

facile,[11] and (2) the rates of ring-closing are slow enough to be followed by ^{1}H NMR but fast enough to be experimentally feasible. We chose ring-closing olefin metathesis rather than ring-opening polymerization or *cis*-2-pentene metathesis because there is only one propagating species, as opposed to the other systems in which more than one propagating species is observed.[4,12] Methylene chloride was found to be a suitable solvent for these studies: ring-closing is approximately three times faster than in benzene, and minimal catalyst decomposition occurs in this solvent.

Catalysts **2a**,**b**,**c**, **3a**,**b**,**c**, **4a**,**b**,**c**, and **5a**,**b**,**c** were synthesized to explore the changes in catalyst activity as the phosphine and halogen ligands are systematically varied. P^iPr_3 has a slightly

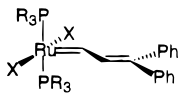

2a: $PR_3{=}PCy_3$, X=Cl
2b: $PR_3{=}PCy_3$, X=Br
2c: $PR_3{=}PCy_3$, X=I
3a: $PR_3{=}PCy_2Ph$, X=Cl
3b: $PR_3{=}PCy_2Ph$, X=Br
3c: $PR_3{=}PCy_2Ph$, X=I
4a: $PR_3{=}P^iPr_3$, X=Cl
4b: $PR_3{=}P^iPr_3$, X=Br
4c: $PR_3{=}P^iPr_3$, X=I
5a: $PR_3{=}P^iPr_2Ph$, X=Cl
5b: $PR_3{=}P^iPr_2Ph$, X=Br
5c: $PR_3{=}P^iPr_2Ph$, X=I

smaller cone angle than PCy_3, but similar electronic properties. On the other hand, P^iPr_2Ph and PCy_2Ph should have cone angles similar to or perhaps slightly smaller than P^iPr_3 and PCy_3, respectively, with substantially different electronic properties than the trialkylphosphines.[13] In this way, the effects of changing the steric or electronic properties of the phosphine can be studied independently. The halogens, on the other hand, pose a more complex problem. While Cl, Br, and I all have different electronic properties, the size of the halogens also varies substantially down the series. Because of this, the effects of the halogens cannot readily be separated into predominantly steric or predominantly electronic in nature. The catalyst activities, measured under a standard set of conditions which provided reasonable rates for study, are summarized in Table 1.

Ligand Effects upon Catalyst Activity. As previously demonstrated by the remarkable difference in reactivities between catalysts **1** and **2a**, it was found that varying the nature of the phosphine ligands resulted in substantial changes in catalyst activity. Catalysts **2a**,**b**,**c** with PCy_3 ligands were found to be more active than the respective catalysts **4a**,**b**,**c** with P^iPr_3 ligands. Likewise, catalysts **3a**,**b**,**c** with PCy_2Ph ligands are more active than the respective catalysts **5a**,**b**,**c** with P^iPr_2-Ph ligands. These results suggest that phosphines with larger cone angles generate catalysts with greater activities.

A more dramatic electronic effect is observed. Catalysts **2a**,**b**,**c** with PCy_3 ligands are much more active than the respective catalysts **3a**,**b**,**c** with PCy_2Ph ligands. Similarly, catalysts **4a**,**b**,**c** with P^iPr_3 ligands are much more active than the respective catalysts **5a**,**b**,**c** with P^iPr_2Ph ligands. Thus, merely changing one cyclohexyl or ispropyl group to a phenyl group—and thereby making the phosphine less electron donating—results in a marked decrease in catalyst activity. This trend is even further illustrated by the fact that **1**, which has PPh_3 ligands, is totally inactive for the metathesis of diethyl diallylmalonate, and will only react with suitably strained olefins.

An interesting trend is observed when the halogens are varied. Comparing catalyst **2a**, **2b**, and **2c**, it is easily seen that going down the series from Cl to Br to I corresponds to a decrease in catalyst activity. It should be noted that in going from Cl to Br, catalyst activity is depressed only slightly, while changing to I has a precipitous effect. Similar effects are observed for catalysts **3**, **4**, and **5**, with catalysts **3c** and **5c** being sufficiently slow that ring-closing is negligible at 20 °C. These observations are puzzling, as they suggest that the more electron withdrawing and smaller halogens generate more active catalysts—trends that are exactly *opposite* to those observed when varying the phosphines.[14]

While consistent trends are observed throughout this series of catalysts, it appears that the steric and electronic effects of the phosphines upon catalyst activity are opposite to those observed for the halogens. *Phosphines, which are larger and more electron donating, and likewise halogens, which are smaller and more electron withdrawing, lead to more active catalysts.*

Mechanism of Olefin Metathesis. Initially, two general mechanisms for olefin metathesis by these catalysts were proposed (Scheme 2). The top pathway, termed "associative" (NOT in the classical ligand-exchange sense), assumes that the olefin simply coordinates to the catalyst to form the intermediate 18-electron olefin complex, followed by the actual metathesis steps to form the product. The bottom pathway, termed "dissociative", assumes that upon binding of the olefin, a phosphine is displaced from the metal center to form a 16-electron olefin complex, which undergoes metathesis to form the cyclized product, regenerating the catalyst upon recoordination of the phosphine. (It should be noted that the "associative" mechanism at first appeared more attractive, because all of the intermediates have either 16 or 18 electrons. In the "dissociative" pathway, all of the intermediates also have either 16 or 18 electrons, with the exception of the 14 electron metallacyclobutane). In order to distinguish between these two mechanisms, the kinetics of the reaction were examined by monitoring product formation (or substrate disappearance) over time.

(11) Bowden, N.; Grubbs, R. H. Unpublished results.

(12) By propagating species, we refer to the resting state of the catalyst as determined by NMR spectroscopy, which is the species $(PR_3)_2X_2Ru{=}CH_2$ in this ring-closing metathesis reaction.

(13) For background reading on the steric and electronic properties of phosphines, see: (a) Brown, T. L.; Lee, K. J. *Coord. Chem. Rev.* **1993**, *128*, 89−116. (b) Wilson, M. R.; Woska, D. C.; Prock, A.; Giering, W. P. *Organometallics* **1993**, *12*, 1742−1752. (c) Tolman, C. A. *Chem. Rev.* **1977**, *77*, 313−348.

(14) The same trend is observed for the polymerization of norbornene by the compounds $(PPh_3)_2X_2Ru{=}CH{-}CH{=}CPh_2$ (X = Cl, Br, I). To further explore the relative electron withdrawing abilities of the X ligands, we synthesized the two compounds $(PPh_3)_2(Cl)(X)Ru{=}CH{-}CH{=}CPh_2$ (X = CH_3CO_2, CF_3CO_2). We found that the trifluoroacetate-containing catalyst polymerized norbornene at least ten times faster than the acetate-containing catalyst, and therefore we conclude that more electron withdrawing X groups produce more active catalysts.

Scheme 2

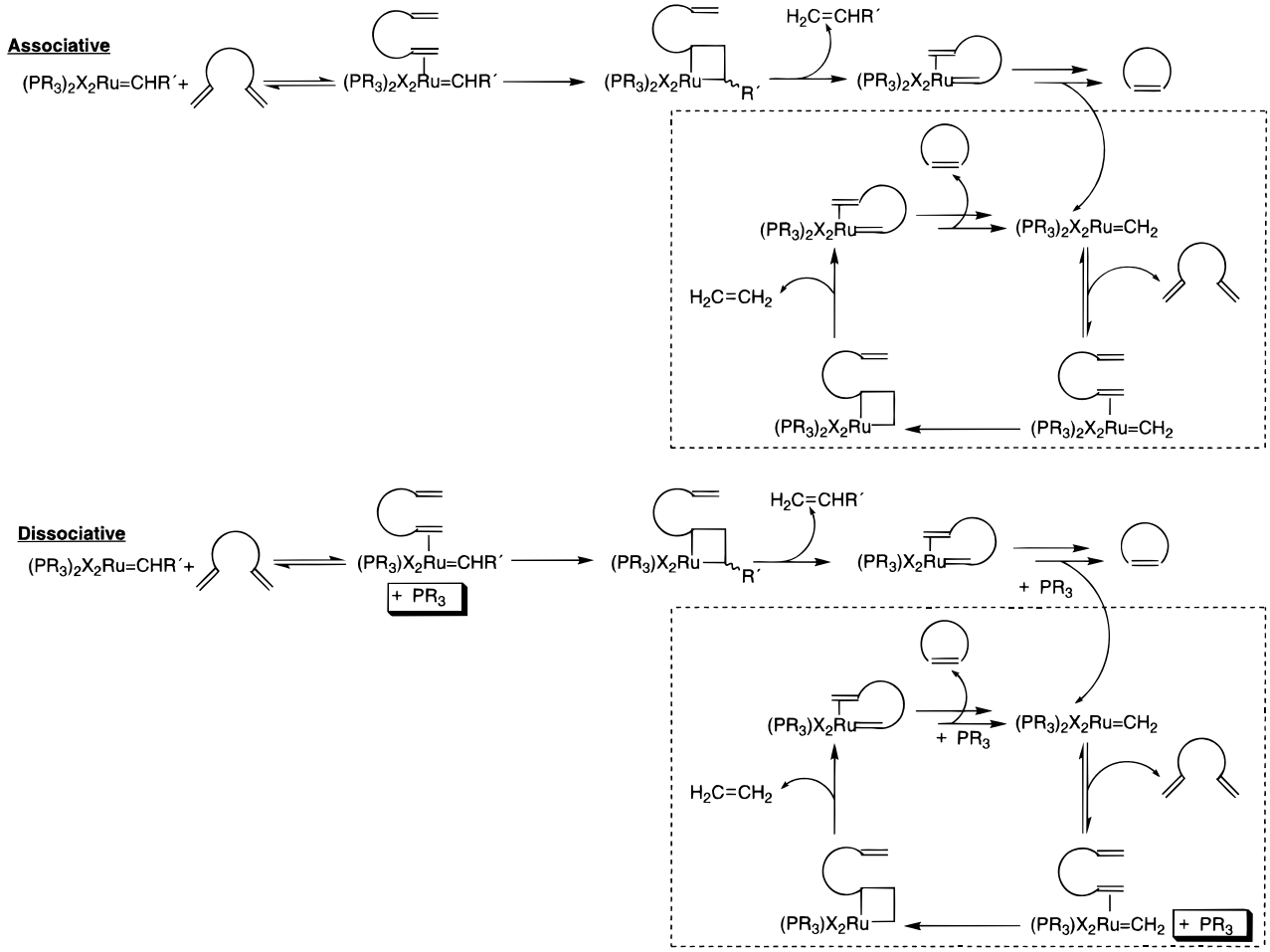

Inspection of the plots of product versus time for the ring-closing reaction with catalysts **2**−**5** indicated that the kinetics did not exhibit first-order behavior with respect to diene. In fact, the curves fit remarkably well to a double-exponential expression, as shown in Figure 1. We considered the possiblity that the unexpected kinetic behavior might be due to differences between the initiating carbene (Ru═CH−CH═CPh_2) and the propagating carbene (Ru═CH_2). The synthesis and isolation of the ruthenium methylidene catalyst **6**,[15] which was used in all of the following kinetic experiments, allowed us to resolve this issue. We observed similar results with catalyst **6**: the

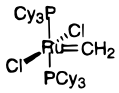

6

kinetics still did not exhibit first-order behavior with respect to the diene, and instead fit very well to a double-exponential expression. These observations led us to conclude that the differences between the initiating and propagating carbenes were not responsible for the unexpected kinetic behavior.

Because the dissociative pathway in Scheme 2 relies on a phosphine dissociating upon olefin binding, we added excess phosphine to the reaction, reasoning that addition of phosphine would disfavor the equilibrium for olefin binding. Likewise, if the associative pathway were active, adding excess phosphine would have little or no effect upon the reaction kinetics. Two important results were obtained from these experiments. First, addition of 0.25−1.0 equiv (0.005−0.020 M) of phosphine (with respect to 0.020 M catalyst) depresses the rate dramatically, with the reaction proceeding up to 20 times slower upon the addition of 1.0 equiv (0.020 M) of phosphine. Second, as shown in Figure 2, the kinetics become *pseudo first order* with respect to diene upon addition of phosphine. This fortuitous result allows us to obtain a pseudo-first-order rate constant k_{obs}, which can be used to determine the relationship between k_{obs} and phosphine concentration. The plot of k_{obs} vs. reciprocal phosphine concentration in Figure 3 shows a linear correlation, and the positive intercept indicates that there is an additional phosphine-independent term in the rate expression.

To determine the complete rate expression for the ring-closing reaction, experiments were conducted to determine the rate dependence upon catalyst concentration. Because of the complex kinetics in the absence of excess phosphine, we could not measure an observed rate constant k_{obs} for the ring-closing reaction under these conditions. The fact that these curves fit to a double-exponential expression was utilized to find the rate at each point in time simply by taking the derivative of the double-exponential curve fit. The plots of rate of diene disappearance vs diene concentration for different catalyst concentrations are shown in Figure 4. The data are obviously not first order—at least not initially. (It appears, however, that the reaction eventually reaches a steady state, which occurs after more than half of the substrate has been consumed.) By comparing these calculated rates at identical diene concentrations, as summarized in Table 2, we find an *approximate* square-root dependence on catalyst concentration.

(15) Schwab, P.; Grubbs, R. H.; Ziller, J. W. *J. Am. Chem. Soc.* **1996**, *118*, 100−110.

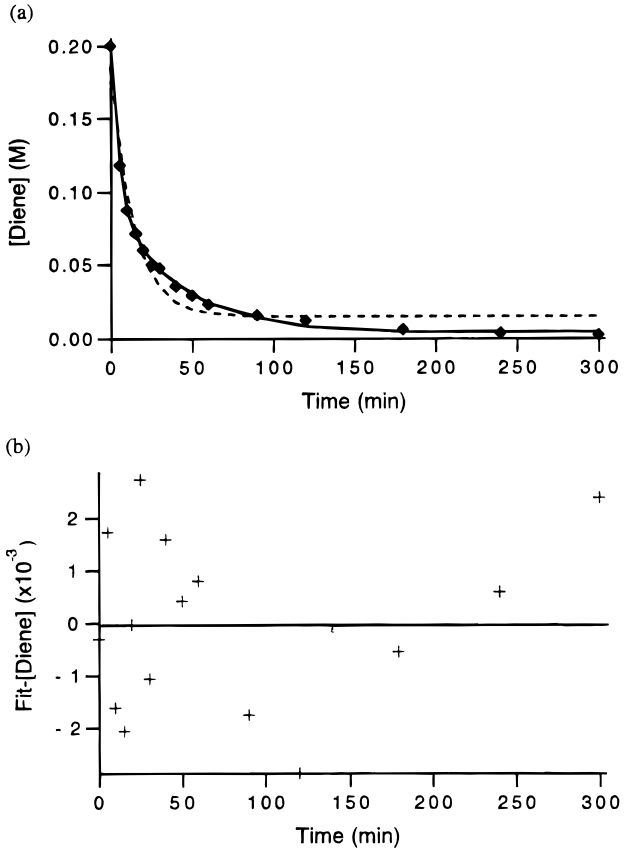

Figure 1. (a) Representative plot of diene concentrations vs time for catalyst **4a**. The reaction was carried out with $[\text{diene}]_0 = 0.2$ M and [catalyst (**4a**)] = 0.01 M in CD_2Cl_2 at 20 °C. The filled diamonds are the data points, and the solid line is the double-exponential fit: $[\text{diene}](t) = K_0 + K_1 \exp(-K_2 t) + K_3 \exp(-K_4 t)$. The dashed line is the best first-order fit $[\text{diene}](t) = K_0 + K_1 \exp(-K_2 t)$. The constants K_n are generic constants that are calculated by the curve-fitting procedure. (b) The residuals (crosses) from the double-exponential fit in part (a) were found by taking the difference between the data and the curve fit at each point.

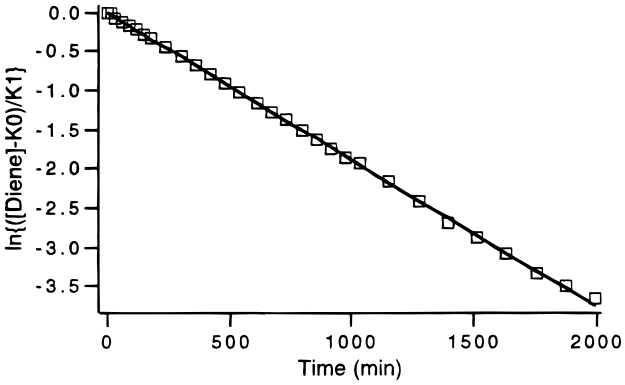

Figure 2. Log plot of diene concentration vs time for the ring-closing metathesis of diethyl diallylmalonate in the presence of 0.02 M PCy_3, where $[\text{Ru}]_0$(**6**) = 0.02 M and $[\text{diene}]_0 = 0.2$ M. The reactions were carried out in CD_2Cl_2 at 30 °C. K_0 and K_1 are the constants from the first-order fit $[\text{diene}](t) = K_0 + K_1 \exp(-K_2 t)$, and K_2 is the slope of the line, where the constants K_n are generic constants calculated by the curve-fitting procedure. The boxes are the data points and the line is the linear fit. Intercept = $(6.45 \pm 7.64) \times 10^{-3}$; slope = $(-1.88 \pm 0.01) \times 10^{-3}$; linear correlation coefficient = 1.00.

Finally, to determine the *actual* catalyst order in the rate expression, the reactions in which the catalyst concentration was varied were repeated in the presence of a constant concentration of excess phosphine. By adding the excess phosphine, the pseudo-first-order rate constants could be obtained. A plot of k_{obs} vs catalyst concentration is shown in Figure 5. A good linear correlation is observed, and it can be concluded that the reaction is first order with respect to catalyst concentration. The final rate expression is shown in eq 1, where k_{obs} is the expression within parentheses, and $[\text{Ru}]_0$ is the concentration of catalyst (i.e., the total concentration of ruthenium in the system).

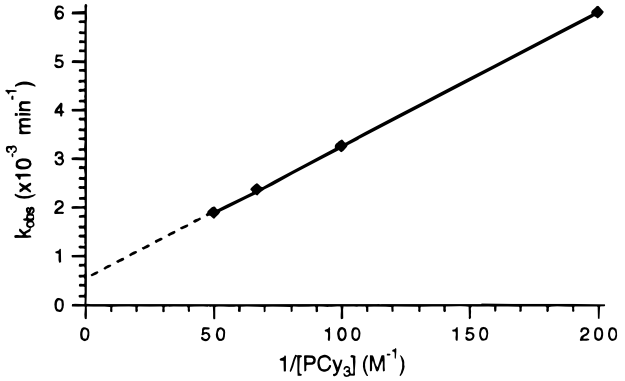

Figure 3. Plot of k_{obs} vs reciprocal phosphine concentration for the ring closing metathesis of diethyl diallylmalonate at varying phosphine concentrations, with $[\text{diene}]_0 = 0.2$ M and $[\text{Ru}]_0$ (**6**) = 0.02 M. The reactions were carried out in CD_2Cl_2 at 30 °C. The filled diamonds are the data points, the solid line is the linear fit $k_{obs} = K_0 + K_1(1/[PCy_3])$, where the constants K_n are generic constants calculated by the curve-fitting procedure, and the dashed line is the extrapolation of the linear fit to the intercept. Intercept = $(5.27 \pm 0.13) \times 10^{-4}$; slope = $(2.73 \pm 0.01) \times 10^{-5}$; linear correlation coefficient = 1.00.

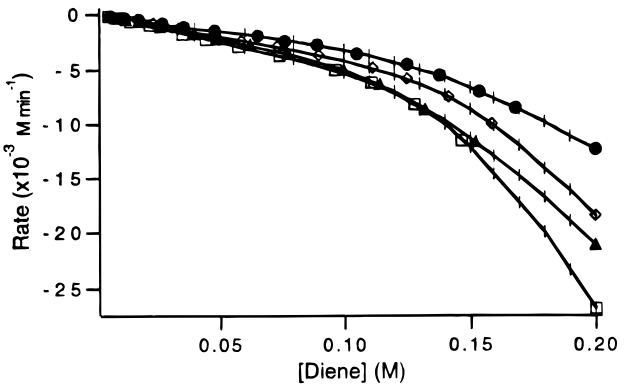

Figure 4. Plot of reaction rate vs diene concentration for the ring-closing metathesis of diethyl diallylmalonate at varying concentrations of catalyst (**6**), with $[\text{diene}]_0 = 0.2$ M. The reactions were carried out at 25 °C in CD_2Cl_2. The data points and concentrations of catalyst **6** are as follows: filled circles, 0.005 M; open diamonds, 0.010 M; filled triangles, 0.015 M; open squares, 0.020 M. The data points were obtained by first fitting the plots of $[\text{diene}](t)$ vs time to the double-exponential expression: $[\text{diene}](t) = K_0 + K_1 \exp(-K_2 t) + K_3 \exp(-K_4 t)$, where the constants K_n are generic constants calculated by the curve-fitting procedure. Using the derivative of this equation and the calculated values for the constants K_n, the rate can be calculated as a function of time. The diene concentration is already expressed as a function of time in the double-exponential relationship above, so the rate can be expressed more usefully as a function of diene concentration, represented by the solid lines in the above figure. The vertical hash marks are the diene concentrations at which the rates were compared, for which the data are summarized in Table 2.

$$-\frac{\mathrm{d}[\text{diene}]}{\mathrm{d}t} = \left(\frac{A}{[PCy_3]} + B\right)[\text{Ru}]_0[\text{diene}] \qquad (1)$$

In order to explain this result, we have proposed a mechanism in Scheme 3 in which both the "associative" and "dissociative"

Table 2. Ratios of Rates for Ring-Closing Metathesis with Varying Catalyst Concentrations

	ratio of catalyst concns		
	(0.010 M)/ (0.005 M)	(0.015 M)/ (0.005 M)	(0.020 M)/ (0.005 M)
average[a]	1.33	1.61	1.81
1σ[b]	0.0741	0.111	0.185
2σ[b]	0.148	0.222	0.370
3σ[b]	0.222	0.333	0.555

[a] The rates of olefin metathesis for different catalyst concentrations were determined at the diene concentrations designated by vertical hash marks in Figure 4. The rates of metathesis for the different catalyst concentrations were then compared at several *identical* diene concentrations (so that the rate dependence on diene concentration cancels out), and the ratios calculated at these diene concentrations were averaged accordingly. Thus, the ratios shown above show the effect of doubling, tripling, and quadrupling (from left to right) the catalyst concentration upon the rate of metathesis. By doubling the catalyst concentration, the rate of metathesis increases by a factor of 1.33; by tripling the catalyst concentration, the rate increases by a factor of 1.61; and by quadrupling the catalyst concentration, the rate increases by a factor of 1.81. This appears to demonstrate an *approximate* square-root dependence upon catalyst concentration, where the rate would increase by a factor of 1.41, 1.73, and 2.00, respectively. [b] σ = standard deviation calculated from the data.

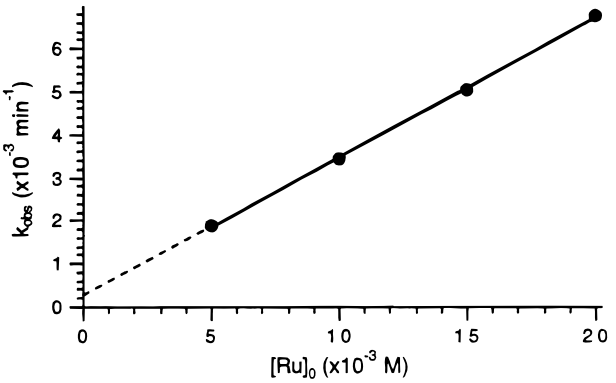

Figure 5. Plot of k_{obs} vs catalyst concentration for the ring-closing metathesis of diethyl diallylmalonate at varying catalyst concentrations in the presence of 0.005M PCy_3, with $[diene]_0 = 0.2$ M. The reactions were carried out in CD_2Cl_2 at 30 °C. The filled circles are the data points, the solid line is the linear fit $k_{obs} = K_0 + K_1([Ru]_0)$ where the constants K_n are generic constants calculated by the curve-fitting procedure, and the dashed line is the extrapolation of the linear fit to the intercept. Intercept $= (2.42 \pm 0.72) \times 10^{-4}$; slope $= 0.323 \pm 0.005$; linear correlation coefficient = 1.00.

pathways from Scheme 2 are operating. Because no intermediates are observed during the course of reaction, the rate of disappearance of diene is equal to the rate of product formation. We assumed that in both cases, metallacycle formation is the rate determining step[16,17]—in the "dissociative" pathway, the metallacyclobutane is a 14-electron complex,[18] and in the "associative" pathway, the metallacyclobutane is a 16-electron complex with a sterically demanding environment—the metallacyclobutane being the highest energy intermediate. The rate of disappearence of diene based on Scheme 3 is shown in eq 2:

$$-\frac{d[diene]}{dt} = k_3[I_2] + k_4[I_1] \quad (2)$$

By solving the equilibria for the concentrations of $[I_1]$ and $[I_2]$, one easily obtains:

$$[I_1] = K_1[\mathbf{6}][diene] \quad \text{and}$$

$$[I_2] = K_2\frac{[I_1]}{[PCy_3]} = K_1K_2\frac{[\mathbf{6}][diene]}{[PCy_3]} \quad (3)$$

Substituting eq 3 into eq 2 yields the final rate expression:

$$-\frac{d[diene]}{dt} = \left(k_3\frac{K_1K_2}{[PCy_3]} + k_4K_1\right)[\mathbf{6}][diene] \quad (4)$$

By comparing eq 4 with the empirical rate expression in eq 1, where $[\mathbf{6}] = [Ru]_0$, we find that the constants A and B are:

$$A = k_3K_1K_2 \quad \text{and} \quad B = k_4K_1 \quad (5)$$

Referring back to eq 1, we can attribute the first part of k_{obs} to the "dissociative" pathway—the rate is inversely proportional to the concentration of unbound phosphine, and directly proportional to the concentrations of both catalyst and diene. The second part of k_{obs} can be attributed to the "associative" pathway—the rate is directly proportional to the concentrations of both catalyst and diene, and independent of the concentration of unbound phosphine. From the data in Figure 3, however, we concluded that B, the observed rate constant for the "associative" pathway, is relatively small compared to the quotient $A/[PCy_3]$, such that in the absence of excess phosphine, the "dissociative" part of the expression clearly dominates (>90−95%).

We can rationalize the kinetic behavior as follows. Because the starting catalyst (with both phosphines) is the only species observed by NMR during the reaction, and likewise no unbound phosphine is observed, we can assume that the amount of unbound phosphine does not exceed 5% of the catalyst concentration. In considering the equilibrium for diene coordination and phosphine dissociation, the concentration of unbound phosphine at every point in time should be proportional to the square root of the catalyst concentration, as shown in Scheme 4. The approximate square-root dependence of the rate on catalyst concentration, observed previously in the absence of added phosphine (Table 2), is consistent with this analysis.

The addition of a mere 0.25−1.0 equiv (0.005−0.020 M) of phosphine (with respect to 0.020 M catalyst) is sufficient to swamp the concentration of unbound phosphine orginating from the catalyst. Because the phosphine concentration is constant, the kinetics become pseudo-first order with respect to diene, as demonstrated by eq 1. Finally, when the catalyst concentration is varied in the presence of added phosphine (and thus keeping a constant phosphine concentration), the linear correlation between k_{obs} and catalyst concentration can be extracted.

Stereochemistry of Intermediates. Before we can consider an explanation for the ligand effects in Table 1, we must first determine the stereochemistry of the postulated intermediates I_1 and I_2 in our proposed mechanism (Scheme 3). Scheme 5 describes what we at first considered to be the two most plausible stereochemical pathways for the "dissociative" pathway in Scheme 3—the "dissociative" pathway, being responsible

(16) It may be argued that breakdown of the metallacycle is the rate determining step, in which case our differential equations are only slightly altered, and still in agreement with our empirically derived rate expression. However, we believe that metallacycle formation is rate determining, as it corresponds to a formal two electron oxidation of the ruthenium center.

(17) We also believe that the second metathesis step, the intramolecular reaction to form the cyclized product is faster than the first, intermolecular metathesis, due to the decreased activation entropy. This is evidenced by the fact that we never observe the intermediate that preceeds the cyclization step even when excess phosphine is added, as opposed to the cyclization of 1,7-octadiene to cyclohexene, during which this intermediate is observed by ^{1}H NMR in the presence of excess phosphine.

(18) The possiblity that the diene chelates the metal center to form a 16-electron complex cannot be ruled out, although entropically this seems unlikely without any predisposition of the diene toward chelation as in the case of butadiene, norbornadiene, or 1,5-cyclooctadiene.

Scheme 3

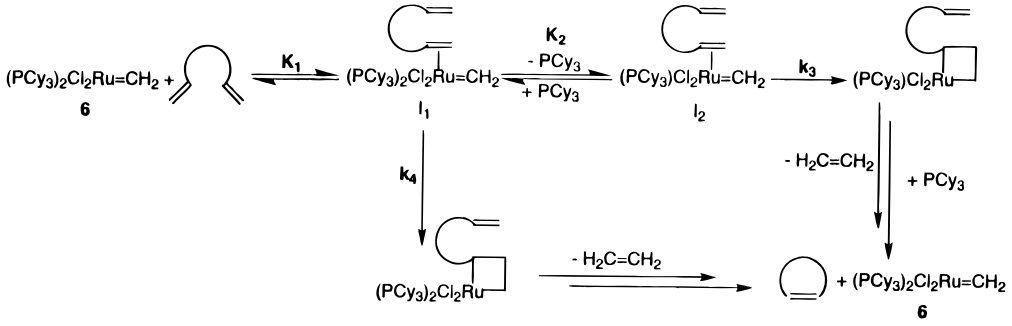

Scheme 4

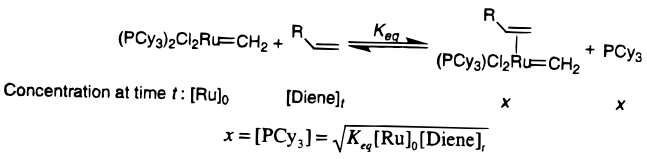

for 95% of catalyst turnover, will also be responsible for the differences in catalyst activity.

From the crystal structures of the vinylcarbene[4] and benzylidene[15] ruthenium catalysts $(PCy_3)_2Cl_2Ru{=}CHR$, we know that they both have a raised square pyramidal geometry with the carbene occupying the apical position. The carbene moiety lies in the Cl−Ru−Cl plane, as opposed to the crystal structure of catalyst **1**[1] in which the carbene moiety lies in the P−Ru−P plane. This is reflected by the coupling constant $^3J_{HP}$ between H_α on the carbene and the phosphorous nuclei in the ^{1}H NMR spectra—$^3J_{HP}$ is approximately zero in the spectrum of the vinylcarbene and benzylidene catalysts $(PCy_3)_2Cl_2Ru{=}CHR$,[4,15] and 11−12 Hz in the spectrum of **1**.[1] From this we conclude that $^3J_{HP}$ closely follows the Karplus relationship for the P−Ru−C_α−H_α dihedral angle.[4]

Because $^3J_{HP}$ is approximately zero in the methylidene catalyst **6**, we have concluded that the carbene moiety lies in the Cl−Ru−Cl plane.[19] Furthermore, because it is necessary that the carbene moiety and olefin approach each other in a face-to-face manner to effect metallacycle formation, the carbene orientation must be considered in our analysis. According to these arguments, an olefin coordinated in one of the positions currently occupied by PCy_3 will be in the required face-to-face orientation with the ruthenium−carbene double bond.

In Scheme 5, pathway 1 depicts olefin coordination *trans* to the carbene to make an 18-electron intermediate I_1, followed by phosphine dissociation with olefin migration to form a 16-electron intermediate I_2 in which the olefin is *cis* to the carbene. Assuming that the carbene retains its orientation, this 16-electron intermediate has the required geometry for metallacyclobutane formation and subsequent metathesis.

Pathway 2 depicts I_1 with the olefin coordinating *cis* to the carbene and chloride migrating to the position *trans* to the carbene. It should be noted that, with the olefin coordinated as shown in I_1 , the carbene must *rotate* 90° before metallacycle formation can occur. Subsequent phosphine dissociation, along with carbene rotation, forms the 16-electron intermediate I_2, which has the required geometry for metallacycle formation.

In a comparison of these two mechanisms, pathway 1 appeared to be more plausible. The olefin coordinates in what appears to be the open coordination site, and phosphine dissociates with olefin migration to a position from which metallacycle formation can occur. However, after examining the proposed intermediates in greater detail, we have concluded that pathway 2 is more likely based on the following analysis.

Although we have not been able to directly observe olefin complexes of the catalysts **2**−**6**, olefin complexes of the compound $(PCy_3)_2Cl_2Ru(CO)$ have been reported in the literature. Carbon monoxide is an excellent model for the carbene moiety—substantial π-bonding is expected for CO bound to an electron rich Ru(II) metal center, such that a CO ligand will occupy the same ruthenium orbitals as the carbene moiety (in either orientation). Olefin complexes of strong π-acids such as acrylonitrile and 1,2-dicyanoethylene bound to $(PCy_3)_2Cl_2$-Ru(CO) have been characterized by IR and ^{31}P NMR spectroscopy, and in all cases the olefin is coordinated as shown below in **7a** and **7b**.[20] In addition, a crystal structure of the ethylene complex **8**[21] depicts an identical ligand geometry, in which the olefin is bound *cis* to the CO ligand. Based on these structures, we believe that the olefin complex I_1 is correctly depicted in pathway 2 (Scheme 5).

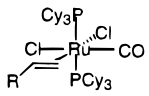

7a: olefin = acrylonitrile
7b: 1,2-dicyanoethylene

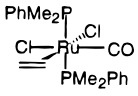

8

Further evidence that the olefin must coordinate *cis* to the carbene moiety is provided by the second step in the ring-closing metathesis reaction (eq 6):

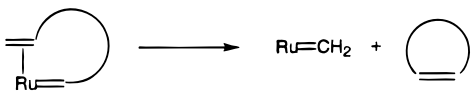

(6)

For small to moderate sized rings, the pendant olefin can only coordinate *cis* to the carbene to which it is tethered—a *trans* coordinated olefin of this type would almost certainly have a prohibitive amount of strain energy. Excepting the unlikely event in which the olefin coordinates in different places depending on whether or not it is tethered to the carbene, these geometric constraints indicate that pathway 2 (Scheme 5) accurately depicts the olefin complex I_1.

For symmetric catalysts such as **1**−**6**, consideration of the principle of microscopic reversibility[22] has interesting consequences for the possible mechanisms of olefin metathesis. For

(19) Chemical exchange decoupling of the phosphines has been ruled out, since the ruthenium-bound phosphine peak is not averaged with the unbound phosphine peak in the ^{31}P NMR spectrum when excess PCy_3 is added. In fact, the ^{1}H and ^{31}P NMR resonances for **6** remain unchanged from 20 to 80 °C in C_6D_6 (catalyst decomposition is significant at this temperature) in both the presence and absence of excess PCy_3, indicating relatively high barriers to both phosphine exchange and carbene rotation.

(20) Moers, F. G.; Langhout, J. P. *J. Inorg. Nucl. Chem.* **1977**, *39*, 591−593.

(21) Brown, L. D.; Barnard, C. F. J.; Daniels, J. A.; Mawby, R. J.; Ibers, J. A. *Inorg. Chem.* **1978**, *17*, 2932−2935.

Scheme 5

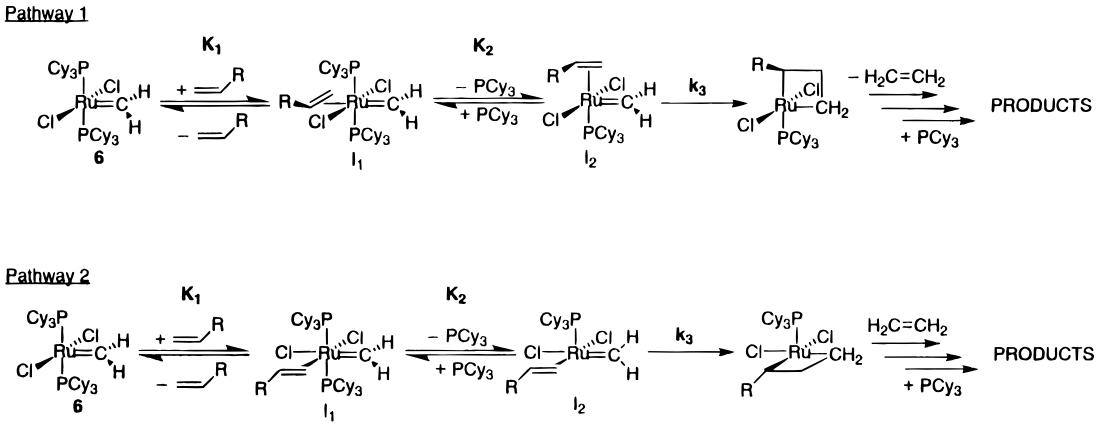

Scheme 6

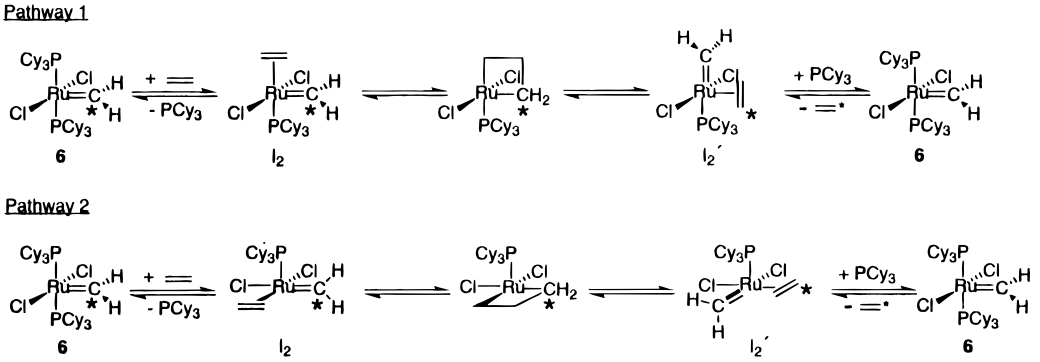

the ruthenium catalysts, it is easiest to consider a degenerate metathesis reaction, as shown in Scheme 6.

According to pathway 1, the square pyramidal intermediate I_2, in which the carbene occupies the apical position and the olefin a basal position, directly precedes metallacyclobutane formation. Productive cleavage of the metallacyclobutane places the carbene in a basal position and the departing olefin in the apical position, intermediate I_2'. In order to regenerate the starting catalyst **6**, some type of ligand rearrangement must occur along with phosphine recoordination and displacement of the product olefin. Because this is a degenerate reaction, the principle of microscopic reversibility requires that the reverse reaction occur at the same rate as the forward reaction. In regarding pathway 1, therefore, two pathways must actually be occurring simultaneously to effect "productive" metathesis—the direct result of having an asymmetric energy profile for a degenerate reaction. The extension of this to nondegenerate olefin metathesis results in there being two competing "dissociative" pathways, which may or may not be kinetically distinguishable from each other.

In pathway 2, on the other hand, formation of the metallacyclobutane from I_2 and subsequent cleavage produces the intermediate I_2', which is actually the enantiomer of I_2. Recoordination of the phosphine and displacement of the product olefin directly regenerates the starting catalyst **6** without the need for any additional ligand rearrangements. Furthermore, because the energy profile is symmetric, no additional pathways are implicated by this mechanism.

When the associative pathway that is implied by the reaction kinetics is also taken into account, pathway 2 becomes even more attractive. In Scheme 3, we have proposed that the olefin complex with two phosphines is a common intermedate in both the associative and dissociative pathways. In pathway 1, however, there is no plausible intermediate that can satisfy both pathways. Either the ligands must rearrange to a species in which the bulky tricyclohexylphosphines are *cis* to each other or an altogether separate pathway must exist in which the olefin coordinates as shown in pathway 2—which in the end provides another reason why pathway 2 is more likely.

By accepting pathway 2 as the more probable mechanism, we are left to rationalize the required 90° carbene rotation that must precede metallacycle formation . This may not be as energetically unfavorable as it may first appear.[19] In catalyst **1**, the conformation of the carbene is already rotated 90° (as compared to **2**–**6**). In compound **9**, the carbene is oriented at a 45° angle such that it bisects the Cl–Ru–Cl and P–Ru–P planes as determined by X-ray crystallography,[3] indicating that linear combinations of the two available π-bonding orbitals on the metal center exist such that the Ru=C π-bond is not broken during the rotation process.

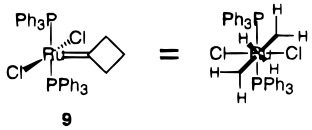

9

Additionally, we have found by ^{1}H NMR spectroscopy that during ligand exchange reactions in which PCy_3 (or another exchangeable phosphine) is added to **1**, the carbene in the mixed phosphine intermediate is oriented as in **1**. It is only upon reaction of the second equivalent of PCy_3 that the carbene rotates. We therefore find it very feasible that, upon dissociation of PCy_3 from the intermediate I_1 in pathway 2, the carbene rotates 90° as the steric and/or electronic environment is changed.

(22) For a brief discussion of the principle of microscopic reversibility, see for example: Laidler, K. J. *Chemical Kinetics*, 2nd ed.; McGraw-Hill: New York, 1965; pp 110–112.

Scheme 7

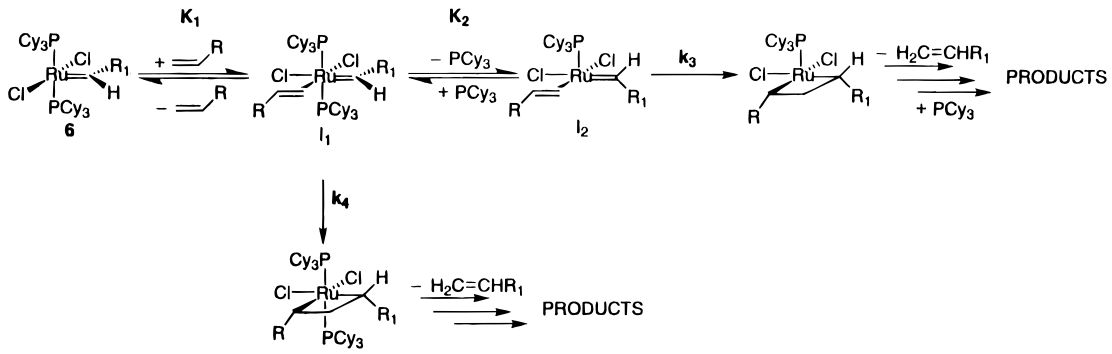

From the above analysis, the preponderance of evidence supports pathway 2 as the more likely mechanism by which the ruthenium catalysts **2**−**6** operate. We have depicted what we propose to be the complete, detailed mechanism in Scheme 7. Based on this, the relationship between the ligand sphere and catalyst activity can be rationalized.

Explanation of Ligand Effects Upon Catalyst Activity. To explain the ligand effects upon catalyst activity, we will refer to the "dissociative" (top) pathway shown in Scheme 7, and eq 7, which is the part of eq 4 that corresponds to the "dissociative" pathway. Because the "dissociative" pathway accounts for approximately 95% of the catalyst turnover, we will ignore the "associative" pathway in our discussion of relative catalyst activities.

$$-\frac{\mathrm{d[diene]}}{\mathrm{d}t} = \left(k_3\frac{K_1K_2}{[\mathrm{PCy_3}]}\right)[\mathbf{6}][\mathrm{diene}] \qquad (7)$$

In deriving eqs 4 and 7, we have assumed that formation of the 14-electron metallacyclobutane intermediate is the rate determining step. All the steps following metallacycle formation should be faster, including intramolecular reaction with the second olefin of the diene to make the cyclic product and regenerate the catalyst. (Independent investigations have confirmed that alkyl-substituted carbenes are more reactive than the unsubstituted methylidene.)[15] From (7), it is easily seen that the rate, and therefore catalyst activity, is directly proportional to three constants: K_1, the equilibrium constant for olefin binding; K_2, the equilibrium constant for phosphine dissociation; and k_3, the rate constant for metallacylobutane formation from the monophosphine olefin complex I_2.

(a) Effect of Halogens. The catalyst activities decrease as the halogens are changed from Cl to Br to I (Table 1). Because the olefin binds *trans* to one of the halogens, their *trans* influencing abilities will have a substantial effect upon the relative ruthenium−olefin bond strengths. The *trans* influence of the halogens increases down the series from Cl to Br to I,[23] so the olefin should be bound *tighest* for Cl and *weakest* for I. Therefore, K_1 will decrease down the series from Cl to I, and we expect a corresponding decrease in the rate. Since *cis* effects are generally weak, phosphine dissociation should not be affected by the change in halogens, and K_2 should remain relatively unchanged. We believe that k_3 also remains relatively unaffected, so an overall decrease in rate, and therefore catalyst activity, will result when changing from Cl to Br to I.

The size of the halogens should also affect the equilibrium for olefin binding. Because the olefin binds *cis* to one of the halogens, we expect that larger halogens such as iodide would disfavor olefin binding due to steric crowding in the halogen−olefin−carbene plane, resulting in a decrease in K_1. By the same reasoning as above, we again predict that catalyst activity will decrease down the series from Cl to I.

(b) Effect of Phosphines. The catalyst activities increase as both the cone angle and the electron donating ability of the phosphines increase. Although these effects are exactly contrary to those observed for the halogens, the proposed mechanism provides a reasonable explanation.

As the cone angle of the phosphine increases, it should be obvious that phosphine dissociation from the sterically crowded 18-electron olefin complex I_1 should be favored, corresponding to an increase in K_2. Although this steric crowding is expected to destabilize I_1, and therefore decrease K_1, the relief of steric crowding should stabilize the monophosphine olefin complex I_2 even further—i.e. bulkier phosphines will favor the overall equilibrium for olefin binding and phosphine dissociation, represented by the product K_1K_2. The product K_1K_2, and hence the rate, is therefore expected to increase as the phosphine cone angle increases.

As the electron donating ability of the phosphines increases, the relative *trans* influence also increases.[24] Because of this, we expect more electron donating phosphines to favor dissociation—by stabilizing the vacant coordination site *trans* to them in the 16-electron monophosphine olefin complex I_2, and especially in the 14-electron metallacyclobutane intermediate. This is analagous to the *trans* effect observed in dissociative ligand substitutions at octahedral metal centers—the rate of substitution increases as the *trans* influence of the appropriate ligand increases, due to weakening of the bond in the ground state and/or stabilization of the five-coordinate intermediate.[24,25] In addition, more electron donating phosphines may facilitate the two-electron oxidation of the metal center to form the metallacyclobutane. This will increase both K_2 and k_3, so we expect the rate to increase substantially as the electron donating ability of the phosphines is increased. The magnitude of these two effects is manifested in the astonishing difference in activity between catalysts **1** and **2a**.

Rate Enhancement by CuCl. The final and perhaps most important aspect of understanding the mechanism of olefin metathesis by these catalysts is the ability to rationally tune catalyst activity in a desired fashion. For example, the rate of metathesis by the ruthenium catalysts is slow compared to that

(23) For a brief discussion of the ligand *trans* influences and the kinetic *trans* effect, see for example: Collman, J. P.; Hegedus, L. S.; Norton, J. R.; Finke, R. G. *Principles and Applications of Organotransition Metal Chemistry*; University Science: Mill Valley, 1987; pp 241−244 and references therein.

(24) Garlatti, R. D.; Tauzher, G. *Inorg. Chim. Acta* **1988**, *142*, 263−267.

(25) (a) Seibles, L.; Deutsch, E. *Inorg. Chem.* **1977**, *16*, 2273−2278. (b) Trogler, W. C.; Stewart, R. C.; Marzilli, L. G. *J. Am. Chem. Soc.* **1974**, *96*, 3697−3699. (c) Tauzher, G.; Dreos, R.; Costa, G.; Green, M. *J. Chem. Soc., Chem. Commun.* **1973**, 413−414. (d) Crumbliss, A. L.; Wilmarth, W. K. *J. Am. Chem. Soc.* **1970**, *92*, 2593−2594.

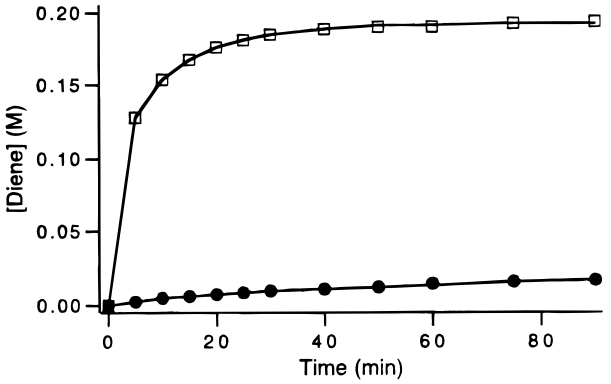

Figure 6. Plot of diene concentrations vs time for catalyst **2c** without (filled circles) and with (open squares) 10 equivalents of CuCl added to the reaction. The reactions were carried out with $[diene]_0 = 0.2$ M and [catalyst (**2c**)] = 0.01 M in CD_2Cl_2 at 20 °C.

of the well-known molybdenum and tungsten alkylidenes,[26] and it would be desirable to tailor the system in such a way as to increase catalyst activity.

With these goals in mind, we wish to report a substantial increase in the rate of olefin metathesis by ruthenium catalysts upon the addition of CuCl. We reasoned that if a "dissociative" pathway accounts for 95% of metathesis in our systems, the equilibrium for phosphine dissociation could be driven by the addition of CuCl, which is known to react with phosphines to make a marginally soluble, ill-defined complex.[27] We found that the addition of 10 equiv of CuCl to a ring-closing reaction effects a rate-enhancement in the case of catalysts **2**−**5**. In some cases, however, the catalyst dies before the reaction goes to >95% completion. The most dramatic effect was observed when CuCl was added to a reaction employing the catalyst $(PCy_3)_2I_2Ru{=}CH{-}CH{=}CPh_2$ (**2c**), shown in Figure 6. In the absence of copper chloride, this catalyst was relatively slow (Table 1). Upon addition of CuCl, however, the activity of this catalyst rivals that of the most active catalyst **2a**, $(PCy_3)_2Cl_2Ru{=}CH{-}CH{=}CPh_2$—an increase by a factor of 20. Furthermore, the addition of CuCl to previously inactive catalysts such as **5c** initiates product formation.[28]

A control experiment employing $CuCl_2$ as the phosphine scavenger was performed, since it is possible that the increase in catalyst activity is due to a redox process involving trace amounts of Cu(II). Because $CuCl_2$ reacts with phosphines in a manner similar to CuCl, we expected either a further increase in catalyst activity if a redox process were operating or a similar increase in catalyst activity if the copper were scavenging the phosphine. We obtained the same results with $CuCl_2$, lending support to the belief that it is the phosphine being taken up by copper, and not a redox process involving Cu(II), that is responsible for the observed rate-enhancement.

The nature of the species generated by adding CuCl to a ruthenium catalyst is unknown. It is possible that a highly reactive, 14-electron monophosphine compound is simply generated, but some recent results suggest that the $CuCl{\cdot}PR_3$ adduct may actually chelate the ruthenium center via bridging chloride ligands. Such bimetallic catalysts with bridging chlorides have been isolated, and are under current investigation.

Conclusions

In exploring the reactivity of many analogous ruthenium catalysts **2**−**5**, some surprising features were uncovered. It was found that the ligand effects upon catalyst activity were exactly opposite for the phosphines and the halogens. *Larger and more electron donating phosphines* produced more active catalysts, while *smaller and more electron withdrawing halogens* likewise produced more active catalysts. These apparently contradictory effects could not be easily explained on the basis of pure steric and/or electronic arguments, prompting further investigation into the mechanism of olefin metathesis by these catalysts.

Mechanistic studies allowed us to formulate an empirical rate equation for the ring-closing of diethyl diallylmalonate by catalyst **6**. The major pathway was found to involve phosphine dissociation from the metal center, such that a minor associative pathway in which both phosphines remain bound can be considered to operate only at higher phosphine concentrations—i.e. when excess phosphine is added to the reaction mixture. We were surprised by the relative importance of the "dissociative" pathway, as it suggests that there is a 14-electron metallacyclobutane intermediate—an electron defficient intermediate for a late transition metal such as ruthenium.

We have concluded that the mechanism in Scheme 7 is in agreement with all of the kinetic evidence, as well as additional evidence found in the literature. The olefin binding site is presumed to be *cis* to the carbene, based upon analagous compounds characterized in the literature employing carbon monoxide in place of the carbene moiety, in addition to the geometric constraints required by the ring-closing metathesis reaction. Furthermore, metallacycle formation and breakdown is thought to occur in a symmetric fashion. If it were to occur in an asymmetric fashion, the mechanism would involve two competing "dissociative" pathways, as well as complex ligand rearrangements about the metal center. One very interesting implication of this mechanism is that in order for metathesis to occur, the carbene must rotate 90° sometime during or after the olefin coordination or phosphine dissociation steps. By using this mechanism as a guide, a self-consistent picture emerges in which the ligand effects can be explained in terms of well-established principles, and a full understanding of the precise nature of metathesis in these systems is gained.

Regarding the "dissociative" pathway, the ligand effects could be rationalized in terms of well-studied systems. Bulkier phosphines favor phosphine dissociation by relief of steric crowding around the ruthenium center. Likewise, the greater *trans* influence of more electron donating phosphines favors phosphine dissociation by stabilizing the 16-electron monophosphine olefin complex, and more importantly the electron defficient 14-electron metallacyclobutane. Halogens, on the other hand, find their primary effects in their relative *trans* influencing abilities. Because the olefin binds *trans* to one of the halogen ligands, more electron withdrawing halogens with a smaller *trans* influence will stablilize the ruthenium−olefin complex. Because the olefin binds *cis* to the other halogen ligand, larger halogens should destabilize the olefin complex due to unfavorable steric crowding.

Finally, reactions were carried out in the presence of CuCl, which is known to complex phosphines. By adding CuCl to the reaction mixture, we hoped to increase the amount of monophosphine species present in the system, and thereby increase the rate of metathesis. Dramatic increases in catalyst activity resulted. The rates of metathesis by slower catalysts

(26) For a discussion of molybdenum and tungsten catalyst activities, see: *Progress in Inorganic Chemistry*; Lippard, S. J., Ed.; Wiley: New York, 1991; Vol. 39, and references therein.

(27) *Comprehensive Coordination Chemistry*; Wilkinson, G., Ed.; Pergamon: New York, 1987; Vol. 5.

(28) It is likely that there is some degree of halogen exchange when catalysts containing Br or I are used. However, complexation of free phosphine is undoubtedly the predominant effect, since Cl-containing compounds such as **2c** are activated by addition of CuCl to the extent that the ring-closing reaction is too fast to study under the standard reaction conditions.

in the presence of CuCl rival that of the fastest catalysts studied, and previously inactive catalysts could now perform the ring-closing reaction. It may be the case that a bimetallic copper−ruthenium species is being formed in these reactions, analagous to other bimetallic catalysts that are currently under investigation.

Experimental Section

All manipulations were performed using standard Schlenk techniques. Argon was purified by passage through columns of BASF R3-11 catalyst (Chemalog) and 4 Å molecular sieves (Linde). Solid organometallic compounds were transferred and stored in a nitrogen-filled Vacuum Atmospheres drybox. All ^{1}H, ^{13}C, and ^{31}P NMR spectra were recorded in CD_2Cl_2 on a JEOL JNM-GX400 (399.80 MHz ^{1}H). All NMR tubes and septa used were dried under vacuum and stored in a drybox.

All solvents were vacuum transferred from sodium benzophenone ketyl, except for chlorinated solvents (including CD_2Cl_2) which were vacuum transferred from CaH_2. All solvents were degassed by several freeze−pump−thaw cycles.

Diethyl diallylmalonate obtained from Aldrich was purified by repeated passage through activated alumina, until all discoloration was gone. The liquid was placed in a Kontes flask with a Teflon stopcock and degassed by several freeze−pump−thaw cycles. The pure, degassed reagent was stored inside the drybox.

Lithium bromide and sodium iodide were dehydrated by placing the solid inside of a large Schlenk flask and heating at 150−160 °C under vacuum overnight. ^{1}H NMR spectra of the salts were obtained in d^8-THF to verify that all excess water had been removed. However, it should be mentioned that water does not harm the reactions or cause catalyst decomposition under reaction conditions.

$(PPh_3)_2Cl_2Ru(CHCHCPh_2)$ was synthesized from $Ru(PPh_3)_4Cl_2$ according to published procedures.[1] The bromine and iodine containing catalysts (**2b**−**5b**, **2c**−**5c**) were synthesized from their chlorine containing analogs (**2a**−**5a**) by Finklestein type chemistry, described below. All catalysts synthesized below can be used without further purification. If necessary, they can be recrystallized from CH_2Cl_2/pentane at low temperature.

Mass spectral analysis was performed at the Southern California Mass Spectrometry Facility at the University of California at Riverside. Elemental analyses were performed by Quantitative Technologies Inc.

Synthesis of $(PCy_3)_2Cl_2Ru(CHCHCPh_2)$ (2a). Inside the drybox, 2.35 g (2.64 mmol) of $(PPh_3)_2Cl_2Ru(CHCHCPh_2)$ (**1**) were weighed into a 150-mL Schlenk flask equipped with stirbar and dissolved in 70 mL of CH_2Cl_2. Tricyclohexylphosphine (2.50 g, 5.35 mmol) were added to the green solution. The flask was capped with a rubber septum, removed from the drybox, placed under argon on the Schlenk line, and stirred overnight at room temperature, during which time the solution changed from green to deep red. The solvent was removed *in vacuo*, and the product was washed liberally with pentane to remove excess phosphines. A small amount of benzene may also be added to help break up the solid. The solid is isolated by cannula filtration, and the washing procedure is repeated. After three or four washes, the remaining red solid is dried in vacuo.

It can easily be determined if there is any remaining starting material **1** by ^{1}H or ^{31}P NMR spectroscopy. If there is any starting material remaining, the above procedure can be repeated (using as much PCy_3 as deemed necessary) until it is all converted to product. The desired product $(PCy_3)_2Cl_2Ru(CHCHCPh_2)$ (2.08 g, 85% yield) was collected and stored inside the drybox. ^{1}H NMR: δ 19.07 (d, 1 H, Ru=C*H*, $^3J_{HH}$ = 11 Hz), 8.68 (d, 1 H, C*H*=CPh$_2$, $^3J_{HH}$ = 11 Hz). ^{31}P NMR: δ 37.59 (s). ^{13}C NMR: δ 289.3 (d of t, Ru=*C*, $^1J_{CH}$ = 150 Hz).

Synthesis of $(PCy_2Ph)_2Cl_2Ru(CHCHCPh_2)$ (3a). The procedure for the synthesis of catalyst **2a** outlined above was followed, with the exception that a larger excess of dicyclohexylphenylphosphine was used (at least 2.5 equiv) and the procedure had to be repeated three times to get complete conversion, due to the poorer equilibrium for phosphine exchange with PPh_3. The product was obtained as a reddish-brown solid. The yields in these cases were typically lower (ca. 60−75%). ^{1}H NMR: δ 19.16 (d, 1 H, Ru=C*H*, $^3J_{HH}$ = 11 Hz), 8.84 (d, 1 H, C*H*=CPh$_2$, $^3J_{HH}$ = 11 Hz). ^{31}P NMR: δ 45.48 (s). ^{13}C NMR: δ 290.9 (d of t, Ru=*C*, $^1J_{CH}$ = 149 Hz). FAB-HRMS: *m/z* calcd for $C_{51}H_{66}Cl_2P_2Ru$ (M^+) 912.3060, found 912.3023.

Synthesis of $(P^iPr_3)_2Cl_2Ru(CHCHCPh_2)$ (4a). The procedure for the synthesis of catalyst **2a** was followed with use of triisopropylphosphine, and the product was obtained as a red solid. ^{1}H NMR: δ 19.19 (d, 1 H, Ru=C*H*, $^3J_{HH}$ = 11 Hz), 8.79 (d, 1 H, C*H*=CPh$_2$, $^3J_{HH}$ = 11 Hz). ^{31}P NMR: δ 46.71 (s). ^{13}C NMR: δ 290.7 (d of t, Ru=*C*, $^1J_{CH}$ = 152 Hz). FAB-HRMS: *m/z* calcd for $C_{33}H_{54}Cl_2P_2Ru$ (M^+) 684.2121, found 684.2126.

Synthesis of $(P^iPr_2Ph)_2Cl_2Ru(CHCHCPh_2)$ (5a). The procedure for the synthesis of **3a** was followed with use of diisopropylphenylphosphine, and the product was obtained as a reddish-brown solid. ^{1}H NMR: δ 19.12 (d, 1 H, Ru=C*H*, $^3J_{HH}$ = 11 Hz), 8.95 (d, 1 H, C*H*=CPh$_2$, $^3J_{HH}$ = 11 Hz). ^{31}P NMR: δ 55.96 (s). ^{13}C NMR: δ 290.5 (d of t, Ru=*C*, $^1J_{CH}$ = 153 Hz). FAB-HRMS: *m/z* calcd for $C_{39}H_{50}Cl_2P_2Ru$ (M^+) 752.1808, found 752.1840.

Synthesis of $(PCy_3)_2Br_2Ru(CHCHCPh_2)$ (2b). Inside the drybox, 200 mg of LiBr were weighed into a small Schlenk flask equipped with a stirbar and dissolved in 1−2 mL of THF. $(PCy_3)_2Cl_2Ru(CHCHCPh_2)$ (**2a**) (100 mg) was then added, followed by 3−4 mL of CH_2Cl_2 . The flask was capped with a rubber septum, removed from the drybox, and stirred for 3−4 h on the Schlenk line under argon at room temperature. The solvents were removed *in vacuo*, and the product was extracted with 3 × 3 mL portions of benzene. The supernatant was collected by cannula filtration into a small Schlenk flask, and the benzene was removed by a freeze-drying procedure in which the flask was placed in a bath of liquid nitrogen to freeze the solution, evacuated, and placed in an ice-water bath. The frozen benzene was sublimed at 0 °C, usually overnight, and the reddish-brown solid was collected and stored inside the drybox. Freeze drying the product in this manner reduces static such that the solid is easily collected. Yields are typically between 90 and 100%. ^{1}H NMR: δ 18.88 (d, 1 H, Ru=C*H*, $^3J_{HH}$ = 11 Hz), 8.79 (d, 1 H, C*H*=CPh$_2$, $^3J_{HH}$ = 11 Hz). ^{31}P NMR: δ 37.82 (s). ^{13}C NMR: δ 291.7 (d of t, Ru=*C*, $^1J_{CH}$ = 152 Hz). Anal. Calcd for $C_{51}H_{78}Br_2P_2Ru$: C, 60.41; H, 7.75. Found: C, 60.66; H, 7.70.

Synthesis of $(PCy_2Ph)_2Br_2Ru(CHCHCPh_2)$ (3b). The procedure for the synthesis of catalyst **2b** was followed with use of 100 mg of $(PCy_2Ph)_2Cl_2Ru(CHCHCPh_2)$ (**3a**), and the product was obtained as a reddish-brown solid. ^{1}H NMR: δ 18.93 (d, 1 H, Ru=C*H*, $^3J_{HH}$ = 11 Hz), 8.91 (d, 1 H, C*H*=CPh$_2$, $^3J_{HH}$ = 11 Hz). ^{31}P NMR: δ 44.81 (s). ^{13}C NMR: δ 293.2 (d of t, Ru=*C*, $^1J_{CH}$ = 149 Hz). FAB-HRMS: *m/z* calcd for $C_{51}H_{66}Br_2P_2Ru$ (M^+) 1002.2030, found 1002.2088.

Synthesis of $(P^iPr_3)_2Br_2Ru(CHCHCPh_2)$ (4b). The procedure for the synthesis of catalyst **2b** was followed with use of 100 mg of $(P^iPr_3)_2Cl_2Ru(CHCHCPh_2)$ (**4a**), and the product was obtained as a reddish-brown solid. ^{1}H NMR: δ 19.03 (d, 1 H, Ru=C*H*, $^3J_{HH}$ = 11 Hz), 8.88 (d, 1 H, C*H*=CPh$_2$, $^3J_{HH}$ = 11 Hz). ^{31}P NMR: δ 46.21 (s). ^{13}C NMR: δ 293.3 (d of t, Ru=*C*, $^1J_{CH}$ = 152 Hz). FAB-HRMS: *m/z* calcd for $C_{33}H_{54}Br_2P_2Ru$ (M^+) 774.1091, found 774.1078.

Synthesis of $(P^iPr_2Ph)_2Br_2Ru(CHCHCPh_2)$ (5b). The procedure for the synthesis of catalyst **2b** was followed using 100 mg of $(P^iPr_2Ph)_2Cl_2Ru(CHCHCPh_2$ (**5a**), and the product was obtained as a reddish-brown solid. ^{1}H NMR: δ 18.94 (d, 1 H, Ru=C*H*, $^3J_{HH}$ = 11 Hz), 9.01 (d, 1 H, C*H*=CPh$_2$, $^3J_{HH}$ = 11 Hz). ^{31}P NMR: δ 54.59 (s). ^{13}C NMR: δ 293.1 (d of t, Ru=*C*, $^1J_{CH}$ = 147 Hz).

Synthesis of $(PCy_3)_2I_2Ru(CHCHCPh_2)$ (2c). Inside the drybox, 200 mg of NaI were weighed into a small Schlenk flask equipped with a stirbar and suspended in 1−2 mL of THF. $(PCy_3)_2Cl_2Ru(CHCHCPh_2)$ (**2a**) (100 mg) was then added, followed by 3−4 mL of CH_2Cl_2 . The flask was capped with a rubber septum, removed from the drybox, and stirred for 4−5 h on the Schlenk line under argon at room temperature. The solvents were removed *in vacuo*, and the product was extracted with 3 × 3 mL portions of benzene. The supernatant was collected by cannula filtration into a small Schlenk flask, and the benzene was removed by the freeze-drying procedure described above for **2b**. The greenish-brown solid was collected and stored inside the drybox. Yields are typically between 90 and 100%. (Note: It has been found that if this reaction is stirred for too long, some catalyst decomposition can occur as evidenced by the appearance of the carbene coupling product Ph_2C=CH−CH=CH−CH=CPh_2 in the ^{1}H NMR spectrum. This can be removed by washing the product with pentane, although care should

be taken as the catalyst is partially soluble in pentane.) ^{1}H NMR: δ 18.54 (d, 1 H, Ru=C*H*, $^3J_{HH}$ = 11 Hz), 8.81 (d, 1 H, C*H*=CPh$_2$, $^3J_{HH}$ = 11 Hz). ^{31}P NMR: δ 38.51 (s). ^{13}C NMR: δ 297.9 (d of t, Ru=*C*, $^1J_{CH}$ = 150 Hz).

Synthesis of (PCy$_2$Ph)$_2$I$_2$Ru(CHCHCPh$_2$) (3c). The procedure for the synthesis of catalyst **2c** was followed with use of 100 mg of (PCy$_2$Ph)$_2$Cl$_2$Ru(CHCHCPh$_2$) (**3a**), and the product was obtained as a greenish-brown solid. ^{1}H NMR: δ 18.52 (d, 1 H, Ru=C*H*, $^3J_{HH}$ = 11 Hz), 8.87 (d, 1 H, C*H*=CPh$_2$, $^3J_{HH}$ = 11 Hz). ^{31}P NMR: δ 42.78 (s). ^{13}C NMR: δ 299.6 (d of t, Ru=*C*, $^1J_{CH}$ = 149 Hz). FAB-HRMS: *m/z* calcd for $C_{51}H_{66}I_2P_2Ru$ (M^+) 1096.1773, found 1096.1817.

Synthesis of (P^{i}Pr$_3$)$_2$I$_2$Ru(CHCHCPh$_2$) (4c). The procedure for the synthesis of catalyst **2c** was followed with use of 100 mg of (P^{i}Pr$_3$)$_2$Cl$_2$Ru(CHCHCPh$_2$) (**4a**), and the product was obtained as a greenish-brown solid. ^{1}H NMR: δ 18.62 (d, 1 H, Ru=C*H*, $^3J_{HH}$ = 11 Hz), 8.84 (d, 1 H, C*H*=CPh$_2$, $^3J_{HH}$ = 11 Hz). ^{31}P NMR: δ 45.74 (s). ^{13}C NMR: δ 299.8 (d of t, Ru=*C*, $^1J_{CH}$ = 152 Hz).

Synthesis of (P^{i}Pr$_2$Ph)$_2$I$_2$Ru(CHCHCPh$_2$) (5c). The procedure for the synthesis of catalyst **2c** was followed with use of 100 mg of (P^{i}Pr$_2$Ph)$_2$Cl$_2$Ru(CHCHCPh$_2$ (**5a**), and the product was obtained as a greenish-brown solid. ^{1}H NMR: δ 18.52 (d, 1 H, Ru=C*H*, $^3J_{HH}$ = 11 Hz), 8.92 (d, 1 H, C*H*=CPh$_2$, $^3J_{HH}$ = 11 Hz). ^{31}P NMR: δ 50.62 (s). ^{13}C NMR: δ 300.1 (d of t, Ru=*C*, $^1J_{CH}$ = 153 Hz).

Ring-Closing Metathesis of Diethyl Diallylmalonate. Reactions for kinetic studies were performed inside the drybox in screw-cap NMR tubes available from Wilmad, sealed with Teflon lined screw caps. Product formation and diene disappearance were monitored by integrating the allylic methylene peaks, using mesitylene as an internal standard.

(1) Relative Catalyst Activity Experiments. A 5X stock solution of the diene was made by diluting 1.21 mL of diethyl diallylmalonate (5 mmol) with 3.79 mL of CD_2Cl_2, with 3.86 μl of mesitylene (5.55 μmol) added as an internal standard, and stored at −40 °C inside the drybox freezer. All reactions were performed inside the drybox by weighing 0.005 mmol of catalyst into the screw-cap NMR tube and dissolving the solid in 400 μL of CD_2Cl_2 added by gas-tight syringe. A 5X diene stock solution (100 μL) was added by gas-tight syringe and the tube was capped, shaken, removed from the drybox, and wrapped with Parafilm. The resulting concentration of catalyst is 0.010 M (1 equiv) and diene is 0.20 M (20 equiv).

(2) Phosphine-Dependence Experiments. Diethyl diallylmalonate was placed in a vial with Teflon lined cap, and 37.2 μL of mesitylene was added. A 5X catalyst stock solution was made immediately prior to use by dissolving 37.3 mg (0.05 mmol) of **6** in 0.5 mL of CD_2Cl_2. A phosphine stock solution was made immediately prior to use by dissolving 14.0 mg of tricyclohexylphosphine (0.05 mmol) in 0.5 mL of CD_2Cl_2. The four reactions were set up simultaneously by adding 30.4 μL of diene/mesitylene solution to either 25, 50, 75, or 100 μL of phosphine solution, and CD_2Cl_2 was added to bring the total volume to 400 μL. Catalyst stock solution (100 μL) was finally added. The NMR tubes were capped, removed from the drybox, wrapped well with Parafilm, and placed in an oil bath preheated to 30 °C. The final concentrations areas follows: diene, 0.20 M (10 equiv); catalyst, 0.020 M (1 equiv); and phosphine, 0.005, 0.010, 0.015, or 0.020 M.

(3) Catalyst-Dependence Experiments (No Phosphine). The diene/mesitylene and catalyst **6** stock solutions were made exactly as above in (2) immediately prior to use. The catalyst stock solution was stored in the drybox freezer in a vial with a Teflon-lined screw cap, and the diene/mesitylene solution was stored in a vial with a Teflon-backed septum screw cap and removed from the drybox. The reactions were performed sequentially as follows. Inside the drybox, 25, 50, 75, or 100 μL of catalyst stock solution were added to the NMR tube, and CD_2Cl_2 was added to bring the volume to 400 μL. The NMR tube was sealed with a Teflon-backed septum screw cap, removed from the drybox, and wrapped well with Parafilm. The diene/mesitylene solution was added via gas-tight syringe immediately before the sample was dropped in the NMR probe, with the temperature preset to 25 °C. The final concentrations are as follows: diene, 0.20 M; and catalyst, 0.005, 0.010, 0.015, or 0.020 M.

(4) Catalyst-Dependence Experiments (Excess Phosphine). The diene/mesitylene, catalyst **6**, and tricyclohexylphosphine stock solutions were made exactly as above in (2) immediately prior to use. The reactions were set up simultaneously by adding 25 μL of phosphine solution to 25, 50, 75, and 100 μL of catalyst solution. CD_2Cl_2 was added to bring the volume to 470 μL, and 30.4 μL of diene/mesitylene solution were finally added. The NMR tubes were capped, removed from the drybox, wrapped well with Parafilm, and placed in an oil bath preheated to 30 °C. The final concentrations are as follows: diene, 0.20 M; phosphine, 0.005 M; and catalyst, 0.005, 0.010, 0.015, or 0.020 M.

Acknowledgment. Support has been provided by the National Science Foundation, Rohm and Haas, and the National Institute of Health.

JA963136Z